NBSIR 73-115

Analysis of The Behavior of a Freely Burning Fire in a Quiescent Atmosphere

J. B. Fang

Center for Building Technology
Institute for Applied Technology
National Bureau of Standards
Washington, D. C. 20234

February 1973

Interim Report

Prepared for
Office of Research and Technology
Department of Housing and Urban Development
Washington, D. C. 20410

NBSIR 73-115

ANALYSIS OF THE BEHAVIOR OF A FREELY BURNING FIRE IN A QUIESCENT ATMOSPHERE

J. B. Fang

Center for Building Technology
Institute for Applied Technology
National Bureau of Standards
Washington, D. C. 20234

February 1973

Interim Report

This report is to be superseded by a future publication which will receive general distribution and should be cited as a reference. Please consult the NBS Office of Technical Information and Publications to obtain the proper citation.

U. S. DEPARTMENT OF COMMERCE, Frederick B. Dent, Secretary

NATIONAL BUREAU OF STANDARDS, Richard W. Roberts, Director

ANALYSIS OF THE BEHAVIOR OF A FREELY BURNING FIRE IN A QUIESCENT ATMOSPHERE

J. B. Fang

A mathematical model which describes the physical and geometrical properties of a turbulent buoyant diffusion flame over a free burning fire has been set up for both axisymmetric and two dimensional cases. The mathematical simulation of the flame consists of a combustion zone near its source and a buoyant plume above and has been developed based on the assumptions of infinitely rapid rate of oxygen-limited combustion reaction and "top-hat" profiles representing vertical distributions of the velocity, temperature, and concentration of the flame gas. Analytical solutions are presented showing the effects of fuel mass-flow rate, physical properties of the fuel and ambient air, and the size and shape of burning area on the general characteristics of a buoyant flame. Experimental data on visible flame heights and flame temperature profiles obtained from burning several different fuels have been satisfactorily correlated by the derived expressions.

1. INTRODUCTION

An understanding of heat transfer rate from the flame emerging above a fuel source is of importance in reduction or elimination of fire hazards in buildings. It is known that the ease of ignition and the rate of fire propagation of the material involved in the burning area strongly depend upon the intensity, size, and duration of the exposing fire. The temperature, velocity, and composition of the gases within the fire plume determine rates of heat transfer to contents or structures in a compartment.

The objectives of this analytical study are (1) to obtain a better understanding of the burning behavior of incidental fires such as those fires which may start in a wastebasket or a piece of furniture and (2) to serve as the basis for prediction of heat transfer rates from the flame to nearby surfaces using fundamental quantities such as the fuel burning rate, heat of combustion of combustible volatiles and the geometry and size of the fuel source. The theoretical results can also provide useful information on the fire induced turbulent ceiling-jet which is applicable to the design and placement of fire detectors and suppressors.

In the experimental phase of this project, the burning characteristics of the contents of wastebaskets and individual

pieces of upholstered furniture were measured. [1] For economy and greater repeatability in subsequent experimental studies, it is planned to use a wood crib array to represent a typical piece of furniture. The proposed model of a burning wood crib array permits (a) direct comparisons to be made with experimental measurements and (b) subsequent extensions to other room geometries and fire spread situations.

The present analysis is concerned with a fire plume that exists over a burning area in the absence of wind. A simplified mathematical model describing the behavior of such turbulent buoyant diffusion flames is presented. This model is an extension of previous studies of buoyant plumes [13] to include the analytical treatment of two-dimensional fire plume and the methods of approach to use a characteristic temperature for defining the visible flame tip, a coefficient to account for radiation effect, two separate entrainment constants for the combustion zone and the convection column, and variable concentrations of combustible volatiles supplied at the flame base. Laboratory experiments of free burning fires have been performed. Data from these experiments as well as those from other investigators [2-9] have been correlated with the derived functional relationships suggested by the model.

2. MATHEMATICAL ANALYSIS

Analysis of the burning characteristics of a buoyant diffusion flame to account for the influence of various degrees of complete combustion in the fuel stream can be accomplished by

using methods similar to those used in previous flame plume studies [10-13].

The mathematical description is concerned with a gaseous mixture of combustible volatiles, combustion products and nitrogen issuing from either an axisymmetric source or a linear source into a stagnant atmosphere. The combustion reaction takes place instantaneously as the unburned gaseous fuel combines with oxygen entrained from the surrounding air. The heat evolved during this chemical reaction raises the flame temperature and the buoyancy of the gases produced in the plume causes them to move upward. At the upper portion of the flame, the combustion reaction is complete and the temperature of the resulting convection column decreases upon further mixing with the entrained ambient air. Thus, a turbulent buoyant diffusion flame may be visualized as a combination of two zones: a combustion zone near its source and a buoyant plume zone above.

In order to derive relevant equations governing the flow within the buoyant flame, the following simplifying assumptions are made:

1. Turbulent flow is fully developed and molecular effects can be considered negligible in comparison with the turbulent transport.

2. Turbulent mixing in axial direction is negligible compared to that in transverse direction.
3. No horizontal pressure variation exists between the flame and the surrounding air.
4. The distributions of the velocity, temperature, and concentration in the transverse direction can be represented by the shape of a "top-hat" profile.
5. The transverse momentum flux due to the entrainment of ambient air is proportional to the local upward momentum flux of the rising flame gas.
6. Ambient air is of uniform density and temperature.
7. The gaseous fuel, combustion products and ambient air are perfect gases with identical values of temperature-independent specific heat. The molecular weight of the combustion products in the buoyant plume zone and the ambient air are equal.
8. In the combustion zone, the combustible volatiles mix with the entrained oxygen and burn instantaneously.
9. Radiative heat transfer can be neglected.

Assumptions 1 to 3 are common to most of the mathematical analyses of buoyancy-controlled turbulent plumes [10, 13-16].

The field of flow in most buoyant flames was found to be unchanging turbulence except in close proximity to the flame base [17,18]. However, this initial laminar zone is relatively small compared with the subsequent turbulent region.

Assumption 2 is not valid for large intense area fires where significant vertical entrainment occurs [19].

The pressure within the plume is assumed constant and equal to its ambient value since the lateral pressure variation due to turbulent transport of momentum in the transverse direction is normally small. [20].

The assumption of "top-hat" profiles for velocity, temperature, and concentration distributions has been widely used to give a reasonably good prediction of the gross behavior of turbulent buoyant flames [10,11,13,15].For a low velocity fuel jet, a temperature profile with a maximum at the flame edge and a local minimum at the flame axis has been reported [20]. The off-center maximum tends to shift to the flame axis as the unburned fuel reacts and the turbulent flame develops. It can be expected that velocity and concentration profiles within the flame plume will be similar to the temperature distribution. Therefore a "top-hat" profile for the mean vertical temperature, velocity, and concentration distributions although over-simplified is a reasonable assumption.

The assumption that the entrainment constant for a turbulent buoyant jet with a density differing from the ambient air is proportional to the square root of the ratio of ambient

density to the average density inside the jet has been supported experimentally [21] and derived theoretically [22].

Most fires in the open are not sufficiently large enough to cause significant variation of the temperature and density of the ambient atmosphere. However, these non-uniformity effects can be included in a manner similar to that used for natural convection column above fires [23-25].

The assumption that the gas mixture inside the flame plume and the surrounding atmosphere consists of ideal gases with identical specific heat and molecular weight may be justified where temperatures are not high enough to produce appreciable dissociation and where the buoyant plume above the combustion zone consists primarily of nitrogen entrained from the ambient air.

The instantaneous mixing and combustion to idealize combustion phenomena is frequently used in mathematical analysis of fire plumes [11,13]. The assumption of perfect mixing and a single step overall reaction with oxygen entrainment as a limiting factor for combustion, is a simplification which seems reasonable as long as the combustible mixture is above its ignition temperature.

The effect of radiation due to the high temperature gases inside the flame is very significant and thus will modify temperature and velocity profiles. Radiative heat transfer within and from a buoyant turbulent plume has been included in analytical treatments with the following assumptions that: the plume is a black body emitter [11], the plume gas is considered as an optically transparent medium [24],that the radiation can be divided into lateral and vertical components [26,27],and the radiating gas is a gray medium and the radiative interchange within the flame can be neglected [10]. All of these assumptions which account for the radiation effect require using numerical techniques to solve the resulting non-linear differential equations. Computer solutions cannot give explicit expressions and tend to be inconvenient for studying the effects of various variables on flame behavior. In order to pursue an analytical solution, radiation is ignored in the present analysis. However, its effect can be approximated by suitably modifying the heat of combustion used in the non-radiative model.

With the preceeding assumptions, the governing equations which describe the combustion zone and buoyant plume zone respectively can be obtained from balances of mass, chemical species, momentum and energy along with the ideal gas law as the equation of state. A vertical flame with a differential

volume around which the conservation equations are written is shown in Figure 1. The flow in vertical flames can be considered as either axially symmetric flow over a circular or a square source, or a two-dimensional flow resulting from a linear fuel source.

2.1 The Combustion Zone

2.1.a Axisymmetric Flow

The continuity equation equates the change in mass flux across the differential volume element with the mass rate of ambient air entrained through the outer surface area of the element.

$$\frac{d(Y^2 \rho u)}{dz} = 2 Y E \sqrt{\frac{\rho}{\rho_a}} \rho_a u \tag{1}$$

The equation of conservation of chemical species states that the change in mass flux of species i across the element is balanced out by the local generation of that species and the transverse transport of that species due to mass entrainment.

$$\frac{d(Y^2 \rho u x_i)}{dz} = Y^2 g_i + 2 Y E \sqrt{\frac{\rho}{\rho_a}} \rho_a u x_{ia} \tag{2}$$

The force balance in the axial direction equates the change in momentum across the differential element with the buoyancy force acting on the element.

$$\frac{d(Y^2 \rho u^2)}{dz} = Y^2 g (\rho_a - \rho) \tag{3}$$

With the assumption of oxygen limited combustion, the change in sensible energy across the differential element is equal to the energy liberated by chemical reaction plus the sensible heat carried in by the entrained surrounding air.

$$\frac{d(y^2 \rho u C_p T)}{dz} = 2yE\sqrt{\frac{\rho}{\rho_a}}\,\rho_a u\left(C_p T_a + \frac{Q_c x_{oa}}{\gamma}\right) \tag{4}$$

Introducing the perfect gas law as the equation of state, this may be expressed in the form

$$\rho T = \frac{P M_c}{R}$$

for the combustion zone

$$\rho_a T_a = \frac{P M_a}{R} \tag{5}$$

for the ambient air into the energy equation (4) yields the following simplified form

$$\frac{d(u y^2)}{dz} = \frac{2E}{\omega}\sqrt{\frac{\rho}{\rho_a}}\,uy \tag{6}$$

where $\omega = \frac{M_c}{M_a}\Big/\left(1 + \frac{Q_c x_{oa}}{\gamma C_p T_a}\right)$ and $\frac{1}{M_c} = \sum_i \frac{x_i}{M_i}$, i denotes species including fuel, O_2, N_2 and combustion products.

The boundary conditions at the flame base are

$$z = 0 \;;\; u = u_0,\; \rho = \rho_0,\; x_i = x_{io} \text{ and } y = y_0 \tag{7}$$

2.1.b Two Dimensional Flow

The corresponding equations expressing conservation of mass, species, momentum, and energy for a two-dimensional diffusion flame are:

$$\frac{d(\rho u y)}{dz} = E\sqrt{\frac{\rho}{\rho_a}}\,\rho_a u \tag{8}$$

$$\frac{d(\rho u y x_i)}{dz} = y g_i + E\sqrt{\frac{\rho}{\rho_a}}\,\rho_a u x_{ia} \tag{9}$$

$$\frac{d(\rho u^2 y)}{dz} = g y(\rho_a - \rho) \tag{10}$$

$$\frac{d(\rho u C_p T y)}{dz} = E\sqrt{\frac{\rho}{\rho_a}}\,\rho_a u\left(C_p T_a + \frac{Q_c x_{oa}}{\gamma}\right) \tag{11}$$

where y is the half width of the flame.

Using the ideal gas law as the equation of state, the energy equation (11) can be rewritten as

$$\frac{d(uy)}{dz} = \frac{E}{\omega}\sqrt{\frac{\rho}{\rho_a}}\,u \tag{12}$$

The boundary conditions for these differential equations are

$$z=0\ ;\ u=u_o,\ \rho=\rho_o,\ x_i=x_{io} \text{ and } y=y_o \tag{13}$$

Introduction of the dimensionaless variables

$$u' = \frac{u}{u_o} \qquad \rho' = \frac{\rho}{\rho_a} \qquad \rho_o' = \frac{\rho_o}{\rho_a}$$

$$y' = \frac{y}{y_o} \qquad z' = \frac{z}{y_o} \qquad T' = \frac{T}{T_a} \tag{14}$$

into the mass balance, conservation of species, force balance and modified energy equation yield the following.

Axisymmetric Flow

$$\frac{d(\rho' u' y'^2)}{dz'} = 2E\sqrt{\rho'}\,u' y' \tag{15}$$

$$\frac{d(\rho' u' y'^2 x_i)}{dz'} = y'^2 G_i + 2E\sqrt{\rho'}\,u' y' x_{ia} \tag{16}$$

$$\frac{d(\rho' u'^2 y'^2)}{dz'} = \frac{(1-\rho')}{F_r} y'^2 \tag{17}$$

$$\frac{d(u' y'^2)}{dz'} = \frac{2E}{\omega}\sqrt{\rho'}\, u' y' \tag{18}$$

Two Dimensional Flow

$$\frac{d(\rho' u' y')}{dz'} = E\sqrt{\rho'}\, u' \tag{19}$$

$$\frac{d(\rho' u' y' x_i)}{dz'} = y' G_i + E\sqrt{\rho'}\, u' x_{ia} \tag{20}$$

$$\frac{d(\rho' u'^2 y')}{dz'} = \frac{(1-\rho')}{F_r} y' \tag{21}$$

$$\frac{d(u' y'^2)}{dz'} = \frac{E}{\omega}\sqrt{\rho'}\, u' \tag{22}$$

with the boundary conditions:

$$u'=1,\ \rho'=\rho_0',\ x_i = x_{io},\ y'=1 \text{ at } z'=0 \tag{23}$$

where $G_i = \dfrac{g_i y_o}{\rho_a u_o}$

$F_r = \dfrac{u_o^2}{g y_o}$ Froude number

The solutions to these governing equations are presented in Appendix A. The dependent variables of primary interest are the flame geometry, and the distributions of temperature and concentrations of the component hot gases along the flame axis.

The ratio of the flame height at which stoichiometric mixing occurs to the source radius or half width may be expressed in terms of the mass flow rate and physical properties of the gaseous fuel:

Axisymmetric Flow

$$H_s' = 1.49 \left[\frac{\omega \left(\frac{\omega}{\rho_o'} + \frac{\gamma x_{50}}{x_{oa}} \right)^2}{E^4 (1-\omega)} \right]^{\frac{1}{5}} N_b^{\frac{2}{5}}$$

Two-Dimensional Flow

$$H_s' = 1.65 \left[\frac{\left(\frac{\omega}{\rho_o'} + \frac{\gamma x_{50}}{x_{oa}} \right)^2}{E^2 (1-\omega)} \right]^{\frac{1}{3}} N_b^{\frac{2}{3}}$$

where $H_s' = \frac{H_s}{Y_o}$ and $N_b = \frac{\dot{m}}{\rho_a \sqrt{g Y_o}}$ (24)

The ratio of flame radius or half-width at any height and at stoichiometric mixing to its source radius or half-width expressed as a function of axial distance are also derived in Appendix A and are respectively stated as follows:

For Axisymmetric Flow

$$Y' = 0.8 \frac{E}{\sqrt{\omega}} z' + 1.19 \frac{E\sqrt{\omega}}{(1-\omega)} \left(\frac{N_b}{\rho_o'} \right)^{\frac{2}{5}}$$

For Two-Dimensional Flow

$$Y' = 0.667 \frac{E}{\sqrt{\omega}} z' + 1.10 \frac{E\sqrt{\omega}}{(1-\omega)} \left(\frac{N_b}{\rho_o'} \right)^{\frac{2}{3}} \quad (25)$$

For Axisymmetric Flow

$$Y_s' = 1.19 \left[\frac{E}{\sqrt{\omega^3 (1-\omega)}} \right]^{\frac{1}{5}} \left[\frac{\left(1 + \frac{\gamma x_{50}}{x_{oa}} \right)^5}{\left(\frac{\omega}{\rho_o'} + \frac{\gamma x_{50}}{x_{oa}} \right)} \right]^{\frac{1}{10}} N_b^{\frac{2}{5}}$$

For Two-Dimensional Flow

$$Y_s' = 1.10 \left[\frac{E}{\sqrt{\omega^3 (1-\omega)}} \right]^{\frac{1}{3}} \left[\frac{\left(1 + \frac{\gamma x_{50}}{x_{oa}} \right)^3}{\left(\frac{\omega}{\rho_o'} + \frac{\gamma x_{50}}{x_{oa}} \right)} \right]^{\frac{1}{3}} N_b^{\frac{2}{3}} \quad (26)$$

The axial distributions of the flame density at any height and for stoichiometric mixing in the combustion zone are found to be separately expressed:

For Axisymmetric Flow

$$\rho' = \omega + (\rho_o' - \omega) \left[0.672 C_x^{\frac{1}{5}} \left(\frac{\rho_o'}{N_b} \right)^{\frac{2}{5}} z' + 1 \right]^{-\frac{5}{2}}$$

For Two-Dimensional Flow

$$\rho' = \omega + (\rho_o' - \omega)\left[0.606\, C_x \left(\frac{\rho_o'}{N_b}\right)^{\frac{2}{3}} z' + 1\right]^{-\frac{3}{2}} \tag{27}$$

$$\rho_s' = \frac{\omega\left(1 + \frac{\gamma x_{so}}{x_{oa}}\right)}{\left(\frac{\omega}{\rho_o'} + \frac{\gamma x_{so}}{x_{oa}}\right)} \tag{28}$$

where: $C_x = \frac{E^4(1-\omega)}{\omega^3}$. and $C_x = \frac{E^2(1-\omega)}{\omega^2}$

The temperature profile in the vertical direction can be obtained readily from the expression for the flame density along with the equation of state for a perfect gas.

For Axisymmetric Flow

$$T' = \left(\frac{\rho_o' T_o' M}{M_o}\right)\left[\frac{\left[0.672\, C_x^{\frac{1}{5}}\left(\frac{\rho_o'}{N_b}\right)^{\frac{2}{5}} z' + 1\right]^{\frac{5}{2}}}{\omega\left[0.672\, C_x^{\frac{1}{5}}\left(\frac{\rho_o'}{N_b}\right)^{\frac{2}{5}} z' + 1\right]^{\frac{5}{2}} + (\rho_o' - \omega)}\right]$$

For Two-Dimensional Flow

$$T' = \left(\frac{\rho_o' T_o' M}{M_o}\right)\left[\frac{\left[0.606\, C_x^{\frac{1}{3}}\left(\frac{\rho_o'}{N_b}\right)^{\frac{2}{3}} z' + 1\right]^{\frac{3}{2}}}{\omega\left[0.606\, C_x^{\frac{1}{3}}\left(\frac{\rho_o'}{N_b}\right)^{\frac{2}{3}} z' + 1\right]^{\frac{3}{2}} + (\rho_o' - \omega)}\right] \tag{29}$$

The dimensionless temperature of the hot gases along the flame axis for stoichiometric mixing is found to be expressed as:

$$T_s' = \frac{\left(\omega T_o' + \frac{\gamma x_{so}}{x_{oa}}\right)}{\omega\left(1 + \frac{\gamma x_{so}}{x_{oa}}\right)} \tag{30}$$

The axial concentration distributions of combustible volatiles and of combustion products within the combustion zone are also derived separately in Appendix A:

For Axisymmetric Flow

$$x_f = \frac{\rho_o'\left(x_{so} + \frac{x_{oa}}{\gamma}\right)}{(\rho_o' - \omega) + \omega\left[0.672\, C_x^{\frac{1}{5}}\left(\frac{\rho_o'}{N_b}\right)^{\frac{2}{5}} z' + 1\right]^{\frac{5}{2}}} - \frac{x_{oa}}{\gamma}$$

For Two-Dimensional Flow

$$x_f = \frac{\rho_o'\left(x_{so} + \frac{x_{oa}}{\gamma}\right)}{(\rho_o' - \omega) + \omega\left[0.606\, C_x^{\frac{1}{3}}\left(\frac{\rho_o'}{N_b}\right)^{\frac{2}{3}} z' + 1\right]^{\frac{3}{2}}} - \frac{x_{oa}}{\gamma} \tag{31}$$

For Axisymmetric Flow

$$x_p = \frac{x_{po}P_o' + \omega\left\{x_{pa} + \left(\frac{\mu_p}{\mu_o}\right)x_{oa}\right\}\left\{\left[0.672\,C_x^{\frac{1}{5}}\left(\frac{P_o'}{N_b}\right)^{\frac{2}{5}}z' + 1\right]^{\frac{5}{2}} - 1\right\}}{(P_o' - \omega) + \omega\left\{0.672\,C_x^{\frac{1}{5}}\left(\frac{P_o'}{N_b}\right)^{\frac{2}{5}}z' + 1\right\}^{\frac{5}{2}}}$$

For Two-Dimensional Flow

$$x_p = \frac{x_{po}P_o' + \omega\left\{x_{pa} + \left(\frac{\mu_p}{\mu_o}\right)x_{oa}\right\}\left\{\left[0.606\,C_t^{\frac{1}{3}}\left(\frac{P_o'}{N_b}\right)^{\frac{2}{3}}z' + 1\right]^{\frac{3}{2}} - 1\right\}}{(P_o' - \omega) + \omega\left\{0.606\,C_t^{\frac{1}{3}}\left(\frac{P_o'}{N_b}\right)^{\frac{2}{3}}z' + 1\right\}^{\frac{3}{2}}} \qquad (32)$$

Nitrogen does not take part in the combustion reaction and its concentration along the flame axis is found to be

For Axisymmetric Case

$$x_N = x_{Na} - \frac{P_o'(x_{Na} - x_{No})}{(P_o' - \omega) + \omega\left[0.672\,C_x^{\frac{1}{5}}\left(\frac{P_o'}{N_b}\right)^{\frac{2}{5}}z' + 1\right]^{\frac{5}{2}}}$$

For Two-Dimensional Case

$$x_N = x_{Na} - \frac{P_o'(x_{Na} - x_{No})}{(P_o' - \omega) + \omega\left[0.606\,C_t^{\frac{1}{3}}\left(\frac{P_o'}{N_b}\right)^{\frac{2}{3}}z' + 1\right]^{\frac{3}{2}}} \qquad (33)$$

The mass fractions of combustion products and mitrogen for stoichiometric mixing are respectively expressed by:

$$x_{ps} = \frac{\left[x_{po} + x_{fo}\left(\frac{\mu_p}{\mu_f}\right) + x_{pa}\left(\frac{\gamma x_{fo}}{x_{oa}}\right)\right]}{\left(1 + \frac{\gamma x_{fo}}{x_{oa}}\right)} \qquad (34)$$

$$x_{Ns} = \frac{\left[x_{No} + x_{Na}\left(\frac{\gamma x_{fo}}{x_{oa}}\right)\right]}{\left(1 + \frac{\gamma x_{fo}}{x_{oa}}\right)} \qquad (35)$$

The sum of the mass fractions of all of the constituents except oxygen within the combustion zone must be unity, on the assumption that oxygen and combustible volatiles do not exist together.

$$x_f + x_N + x_p = 1 \qquad (36)$$

2.2 The Buoyant Plume

Chemical reaction is assumed to be terminated at the upper end of the combustion zone and no heat is generated within the convection plume. Thus, the convection plume above the combustion zone behaves as a turbulent buoyant plume which gradually cools upon mixing with the entrained ambient air.

2.2.a Axisymmetric Flow

Referring to the differential volume element of a buoyant flame shown in Figure 1, the equations of conservation of mass and momentum are identical to those describing the combustion zone.

$$\frac{d(Y^2 \rho u)}{dz} = 2Y E' \sqrt{\frac{\rho}{\rho_a}}\, \rho_a u \tag{37}$$

$$\frac{d(Y^2 \rho u^2)}{dz} = Y^2 g (\rho_a - \rho) \tag{38}$$

Because there is no combustion reaction occurring and the hot gases inside the plume and those in the ambient atmosphere are assumed ideal, the conservation equations of species and energy are reduced to the following form:

$$\frac{d(Y^2 \rho u x_i)}{dz} = 2Y E' \sqrt{\frac{\rho}{\rho_a}}\, \rho_a u x_{ia} \tag{39}$$

$$\frac{d(Y^2 \rho u C_p T)}{dz} = 2Y E' \sqrt{\frac{\rho}{\rho_a}}\, \rho_a u C_p T_a \tag{40}$$

Using the ideal gas law to modify the energy equation gives

$$\frac{d(uy^2)}{dz} = 2E'\sqrt{\frac{\rho}{\rho_a}}\,uy \tag{41}$$

2.2.b Two Dimensional Flow

The equations of conservation of mass, momentum, chemical species and energy for the two-dimensional case are:

$$\frac{d(\rho u y)}{dz} = E'\sqrt{\frac{\rho}{\rho_a}}\,\rho_a u \tag{42}$$

$$\frac{d(\rho u^2 y)}{dz} = gy(\rho_a - \rho) \tag{43}$$

$$\frac{d(\rho u y \chi_i)}{dz} = E'\sqrt{\frac{\rho}{\rho_a}}\,u\chi_{ia} \tag{44}$$

$$\frac{d(\rho u y C_p T)}{dz} = E'\sqrt{\frac{\rho}{\rho_a}}\,\rho_a u C_p T_a \tag{45}$$

The energy balance can be simplified with the use of the perfect gas law

$$\frac{d(uy)}{dz} = E'\sqrt{\frac{\rho}{\rho_a}}\,u \tag{46}$$

The boundary conditions at the source of this zone are:

$$z = H_s \;;\; u = u_s \,,\; \rho = \rho_s \,,\; \chi_i = \chi_{is} \text{ and } y = y_s \tag{47}$$

Defining the dimensionless quantities:

$$y^* = \frac{y}{y_s} \quad z^* = \frac{z}{y_s} \quad z_s^* = \frac{H_s}{y_s} \quad u^* = \frac{u}{u_s}$$
$$\rho' = \frac{\rho}{\rho_a} \quad \rho_s' = \frac{\rho_s}{\rho_a} \quad T' = \frac{T}{T_a} \quad T_s' = \frac{T_s}{T_a} \tag{48}$$

and introducing these variables into the conservation equations yields:

Axisymmetric Flow

$$\frac{d(\rho' u^* y^{*2})}{dz^*} = 2E'\sqrt{\rho'}\, u^* y^* \tag{49}$$

$$\frac{d(\rho' u^* y^{*2} x_i)}{dz^*} = 2E'\sqrt{\rho'}\, u^* y^* x_{ia} \tag{50}$$

$$\frac{d(\rho' u^{*2} y^{*2})}{dz^*} = \frac{(1-\rho')}{F_s}\, y^{*2} \tag{51}$$

$$\frac{d(u^* y^{*2})}{dz^*} = 2E'\sqrt{\rho'}\, u^* y^* \tag{52}$$

Two-Dimensional Flow

$$\frac{d(\rho' u^* y^*)}{dz^*} = E'\sqrt{\rho'}\, u^* \tag{53}$$

$$\frac{d(\rho' u^* y^* x_i)}{dz^*} = E'\sqrt{\rho'}\, u^* x_{ia} \tag{54}$$

$$\frac{d(\rho' u^{*2} y^*)}{dz^*} = \frac{(1-\rho')}{F_s}\, y^* \tag{55}$$

$$\frac{d(u^* y^*)}{dz^*} = E'\sqrt{\rho'}\, u^* \tag{56}$$

With the boundary conditions

$$u^* = 1,\ \rho' = \rho'_s,\ x_i = x_{is},\ y^* = 1 \quad \text{at} \quad z^* = z^*_s \tag{57}$$

where: $F_s = \dfrac{u_s^2}{g y_s}$

The solutions to these governing equations for both axisymmetric and two-dimensional cases are given in Appendix B. One of the particular quantities of interest is the flame height which is equal to the sum of the height at which stoichiometric reaction takes place plus the height at which the temperature on the centerline is reduced to a certain value. This total flame height is been derived to be:

For Axisymmetric Flow

$$\frac{H}{Y_o} = (1.49 + 0.916\, K_a^{\frac{1}{5}})\, P_a^{\frac{1}{5}}\, N_b^{\frac{2}{5}}$$

For Two-Dimensional Flow

$$\frac{H}{Y_o} = (1.65 + K_t^{\frac{1}{3}})\, P_t^{\frac{1}{3}}\, N_b^{\frac{2}{3}}$$

(58)

where

$$K_a = \frac{\phi^4 (1-\omega)\left\{\left[\frac{\omega(1-\rho_o')}{\rho_o'} + \frac{\gamma x_{fo}(1-\omega)}{x_{oa}}\right] T_f' + \frac{\omega(\rho_o' T_o' - 1)}{\rho_o'}\right\}^3}{\omega^3 \left(\frac{\omega}{\rho_o'} + \frac{\gamma x_{fo}}{x_{oa}}\right)^3 (1-\rho_s')(T_f'-1)^3}$$

$$P_a = \frac{\omega\left(\frac{\omega}{\rho_o'} + \frac{\gamma x_{fo}}{x_{oa}}\right)^2}{E^4 (1-\omega)}$$

$$K_t = \frac{\phi^2 (1-\omega)\left\{\left[\frac{\omega(1-\rho_o')}{\rho_o'} + \frac{\gamma x_{fo}(1-\omega)}{x_{oa}}\right] T_f' + \frac{\omega(\rho_o' T_o' - 1)}{\rho_o'}\right\}^3}{\omega^2 \left(\frac{\omega}{\rho_o'} + \frac{\gamma x_{fo}}{x_{oa}}\right)^3 (1-\rho_s')(T_f'-1)^3}$$

$$P_t = \frac{\left(\frac{\omega}{\rho_o'} + \frac{\gamma x_{fo}}{x_{oa}}\right)^2}{E^2 (1-\omega)}$$

$$\phi = \frac{E}{E'}$$

These equations indicate that for given fuel volatiles, the ratio of the height of a turbulent, buoyancy-controlled diffusion flame above an axisymmetric source or a linear fuel source to the radius or half-width of the source is directly proportional to the burning rate ($\dot{m}/\rho_a\sqrt{g}Y_o$) raised to the two-fifths and two-thirds powers, respectively.

The ratio of flame radius or half-width to that at the flame base in terms of axial distance for the buoyant plume zone is expressed approximately as

For Axisymmetric Flow

$$Y' = 1.2\,E'(z' - H_s') + 1.1\,C_D^{\frac{1}{5}} N_b^{\frac{2}{5}}$$

For Two-Dimensional Flow

$$Y' = E'(z' - H_s') + C_D^{\frac{1}{3}} N_b^{\frac{2}{3}}$$

where $C_D = \dfrac{E'\left(\frac{\omega}{\rho_o'} + \frac{\gamma x_{so}}{x_{oa}}\right)^2}{\omega^2(1-\rho_s')}$ (59)

Another quantity required for derivation of vertical temperature distribution within the convection plume is the profile of plume density which is found to be:

For Axisymmetric Flow

$$\rho' = 1 - (1-\rho_s')\left[1.09\,E'\,C_D^{-\frac{1}{5}} N_b^{-\frac{2}{5}}(z' - H_s') + 1\right]^{-\frac{5}{3}}$$

For Two-Dimensional Flow

$$\rho' = 1 - (1-\rho_s')\left[E'\,C_D^{-\frac{1}{3}} N_b^{-\frac{2}{3}}(z' - H_s') + 1\right]^{-1} \quad (60)$$

The vertical temperature distribution of plume gas within the convection column can be obtained immediately from the plume density profile and the ideal gas law.

For Axisymmetric Flow

$$T' = \left(\frac{\rho_s' T_s' M}{M_s}\right) \frac{\left[1.09\, E' C_D^{-\frac{1}{5}} N_b^{-\frac{2}{5}} (z' - H_s') + 1\right]^{\frac{5}{3}}}{\left\{\left[1.09 E' C_D^{-\frac{1}{5}} N_b^{-\frac{2}{5}} (z' - H_s') + 1\right]^{\frac{5}{3}} - (1 - \rho_s')\right\}}$$

For Two-Dimensional Flow

$$T' = \left(\frac{\rho_s' T_s' M}{M_s}\right) \frac{\left[E' C_D^{-\frac{1}{3}} N_b^{-\frac{2}{3}} (z' - H_s') + 1\right]}{\left\{\left[E' C_D^{-\frac{1}{3}} N_b^{-\frac{2}{3}} (z' - H_s') + 1\right] - (1 - \rho_s')\right\}} \qquad (61)$$

At height above the stoichiometric mixing plane, the fuel volatiles vanish and the oxygen content (χ_o) along the flame axis may be expressed as:

For Axisymmetric Flow

$$\chi_o = \frac{\chi_{oa}\left\{\left[1.09 E' C_D^{-\frac{1}{5}} N_b^{-\frac{2}{5}} (z' - H_s') + 1\right]^{\frac{5}{3}} - 1\right\}}{\left\{\left[1.09 E' C_D^{-\frac{1}{5}} N_b^{-\frac{2}{5}} (z' - H_s') + 1\right]^{\frac{5}{3}} - (1 - \rho_s')\right\}}$$

For Two-Dimensional Flow

$$\chi_o = \frac{\chi_{oa}\left\{\left[E' C_D^{-\frac{1}{3}} N_b^{-\frac{2}{3}} (z' - H_s') + 1\right] - 1\right\}}{\left\{\left[E' C_D^{-\frac{1}{3}} N_b^{-\frac{2}{3}} (z' - H_s') + 1\right] - (1 - \rho_s')\right\}} \qquad (62)$$

The concentration distribution of combustion products within the hot gas is found to be:

For Axisymmetric Flow

$$\chi_p = \frac{(\chi_{ps} \rho_s' - \chi_{pa}) + \chi_{pa}\left[1.09 E' C_D^{-\frac{1}{5}} N_b^{-\frac{2}{5}} (z' - H_s') + 1\right]^{\frac{5}{3}}}{\left\{\left[1.09 E' C_D^{-\frac{1}{5}} N_b^{-\frac{2}{5}} (z' - H_s') + 1\right] - (1 - \rho_s')\right\}}$$

For Two-Dimensional Flow

$$\chi_p = \frac{(\chi_{ps} \rho_s' - \chi_{pa}) + \chi_{pa}\left[E' C_D^{-\frac{1}{3}} N_b^{-\frac{2}{3}} (z' - H_s') + 1\right]}{\left\{\left[E' C_D^{-\frac{1}{3}} N_b^{-\frac{2}{3}} (z' - H_s') + 1\right] - (1 - \rho_s')\right\}} \qquad (63)$$

The axial distribution of nitrogen content inside the convection plume is also derived in Appendix B and is expressed as:

For Axisymmetric Flow

$$\chi_N = \frac{(\chi_{NS}\rho_s' - \chi_{Na}) + \chi_{Na}\left[1.09\,E'C_D^{-\frac{1}{5}}N_b^{-\frac{2}{5}}(z'-H_s') + 1\right]^{\frac{5}{3}}}{\left\{\left[1.09\,E'C_D^{-\frac{1}{5}}N_b^{-\frac{2}{5}}(z'-H_s') + 1\right]^{\frac{5}{3}} - (1-\rho_s')\right\}}$$

For Two-Dimensional Flow

$$\chi_N = \frac{(\chi_{NS}\rho_s' - \chi_{Na}) + \chi_{Na}\left[E'C_D^{-\frac{1}{3}}N_b^{-\frac{2}{3}}(z'-H_s') + 1\right]}{\left\{\left[E'C_D^{-\frac{1}{3}}N_b^{-\frac{2}{3}}(z'-H_s') + 1\right] - (1-\rho_s')\right\}} \qquad (64)$$

The sum of the mass fractions of oxygen, nitrogen, and combustion products within the hot gas plume must be in unity since all volatile fuels are burned to stoichiometric completion in the combustion zone.

These equations (equations 57 to 61) along with the corresponding results in the combustion zone (equations 24 to 35) provide the shape and size of the visual flame and the profiles of the temperature and species concentration of hot gases throughout the entire flame plume. These quantities are necessary information for estimating the heat transfer rate from the overhead flame of a free-burning fire.

3. Comparison with Experimental Data

The mathematical analysis indicates that the behavior of turbulent buoyancy controlled flames in an unconfined atmosphere depends upon fuel burning rate, shape of the burning area, fuel properties and ambient conditions. The flame height for a given

fuel type can be predicted as a function of burning rate using equation (58), which when plotted on log-log coordinates and in the appropriate dimensionless groups (H/Y_o versus N_b) gives straight line with slopes of 2/5 and 2/3 for the axisymmetric and two dimensional cases, respectively.

The visible flame height and fuel burning rate data obtained from burning cribs of wood sticks arranged on a square base [6], spreading of fires along long wood cribs [7], open trays of liquid fuels [8] and gaseous fuels emerging from various burner shapes and sizes [5,9] have been previously reported. These data along with those obtained recently at NBS with square-based wood cribs are correlated and presented in Figure 2 where H/Y_o is plotted against the modified Froude number ($N_b = \dot{m}/\rho_a\sqrt{g Y_o}$). All of the flame heights shown in the figure were measured from the base of the crib or the top of the burner. The flame rising vertically from a long strip with a source length to width ratio greater than 1.5 were treated as a two-dimensional condition. The density of ambient air and the specific heat of flame gas used in all calculations are assumed to be 1.3×10^{-3} g/cm^3 and 0.24 cal/g ^{o}C respectively. It can be seen from Figure 2 that for a given fuel type or crib design, all the data in each group fall adjacent to a straight line calculated by the method of least squares. Table 1 summarizes the results of

correlation of flame height to rate of burning and fuel source characteristics. As one would expect the value of coefficient K is dependent upon the shape and size of the burning area, the type of fuels involved and the fuel bed structure. The flame heights of the crib fires made recently at NBS are significantly shorter than those by Fons et al. [7] and Gross [6] as illustrated in Table 1. This discrepancy may be due to a large clearance present between the crib base and the platform support, which allows more air to enter the combustion zone through the crib bottom.

Also included in Table 1 are the computed values of dimensionless flame tip temperatures obtained from equation 58 using the values of coefficient K, average entrainment constant for both combustion and buoyant plume zones and fuel properties. The numerical values of the fuel properties used for the calculation of flame tip temperature are listed in Table 2.

The pyrolysis of wood involves various complex processes and the composition of volatile matter evolving from pyrolysis reaction varies considerably depending upon the conditions of external heating and the extent of degradation [28]. Roberts [29] conducted ultimate analyses with partially decomposed wood and observed that over a wide range of volatilization, the mean composition of the volatiles can be represented

by formaldehyde. In the present analysis, gaseous formaldehyde has been used to represent the average pyrolysis product of wood as employed in a previous paper [30].

Table 1 illustrates that the computed flame tip temperature for each data set ranges from 290° to 340°C for crib fires and 400° to 440°C for fires with liquid and gaseous fuels. These values are reasonably consistent with the measured values given in the literature [3, 8, 9]. It may be noted that the values of the entrainment constant (E) used for crib fires to obtain the temperature of flame tip depend upon the construction of the cribs and ventilation conditions at the crib edge. A value for the entrainment constant for buoyant flames from gaseous fuels of E=0.14 gave the best fit to the observed flame tip temperature.

Calculations based on equations 29 and 61 have been made for the distribution of temperature along the flame axis for the fires above a square base crib and a pan of n-heptane. The results of the computations are presented in Figures 3 and 4 where the ratio of the flame temperature to the ambient temperature is plotted against normalized vertical distance from the flame base. Also shown for comparison are the experimental data reported by Tarifa et al [8] and those obtained by the author. Results shown in Figure 3 are based on the idealized condition

that all the gaseous fuel produced from pyrolyzing wood can be visualized as being supplied at the crib base.

As shown in Figures 3 and 4, reasonably good agreement has been found between theoretical predictions and experimental measurements. It may be noted that the best fit value of entrainment constant for the combustion zone differs significantly from that for the buoyant plume. Considering the difference in nature of the two zones and the close agreement with experimental results, the use of two separate entrainment constants for a diffusion flame seems relavant. A recent article [31] has reported that the local entrainment of an axisymmetric turbulent air jet increases with increasing vertical distance in the initial region and then becomes constant in the fully developed flow region which is located an axial distance of approximately fifteen nozzle diameters. This experimentally observed non-uniformity of air entrainment at the early stage of a free jet may also occur in a buoyant flame. Values of the plume zone entrainment constant determined from crib and n-heptane burnings are comparable with a value, $E'=0.08$ reported in a previous paper [21].

The average molecular weight and mass fractions of constituent gases within a flame as a function of normalized axial distance for crib and n-heptane fires are computed by use of equations

31 to 36 and 62 to 64 and the results are presented in Figures 5 and 6 respectively. Values for carbon dioxide and water vapor are obtained from the complete combustion of the gaseous fuel. As shown in the figures, all of the gaseous fuel supplied at the base of the flame are completely consumed at the stoichiometric mixing point and the peak temperature also occurs at this height. It can be seen that the value of mean molecular weight of the flame gas in the buoyant plume region is nearly equal to that for ambient air.

4. Conclusions

The behavior of buoyant diffusion flames above a naturally occurring fire can be predicted by the postulated mathematical model based on a number of simplifying assumptions.

The flame heights of radially symmetric and linear diffusion flames for several different fuels have been correlated reasonably well with the derived parameters describing the fuel source characteristics and fuel properties. From the results of the correlation, the temperature at the visible flame tip defined as the point at which the flame temperature falls to a characteristic value, has been found to range from 290° to 340°C for cribs and 400° to 440°C for gaseous and liquid fuels and are in good agreement with experimental measurements.

The measured temperature profiles along the flame axis for radially symmetric fires are found to agree with theoretical predictions.

It is believed that the gross feature of fire plume such as the flame shape and the vertical distributions of temperature and gas composition can be predicted, using the present model or one similar in nature, for the stated condition of size and shape of burning area and rate of production of pyrolysis products.

TABLE 1

Values of Coefficient K and Exponent n for the Modified Form of Equation 58 ($H/y_o = K N_b^n$) and Flame Tip Temperature

Data Source	Fuel Type	The Length to Half-width (or Radius) Ratio of the Fuel Source	Coefficient K	Exponent n	Flame Tip Temperature T_t/T_a	Average Entrainment Constant $\bar{E}$
Gross (6)	Wood Crib (Douglas Fir)	$\frac{1}{y_o} = 2$	41	2/5	2.05	0.11
Fons et al. (7)	Wood Crib (White Fir)	$\frac{1}{3} < \frac{1}{y_o} < 3$	35	2/5	1.89	0.14
		$3 < \frac{1}{y_o}$	82	2/3	2.01	0.14
Thomas (2)	Wood Crib (white pine)	$3 < \frac{1}{y_o}$	63	2/3	1.92	0.22
This Study	Wood Crib (Hemlock)	$\frac{1}{y_o} = 2$	26	2/5	1.94	0.20
Putnam and Speich (5)	City Gas	$\frac{1}{y_o} = 2$	60	2/5	2.32	0.14
		$2\times10^3 < \frac{1}{y_o} < 4\times10^3$	105	2/3	2.37	0.42
Grinberg and Putnam (9)	Ethane + $1.184N_2$	$\frac{1}{y_o} = 2$	41	2/5	2.38	0.14
Tarifa et al.(8)	n-Heptane	$\frac{1}{y_o} = 2$	36	2/5	2.25	0.21

TABLE 2

VALUES OF THE FUEL PROPERTIES USED

FOR FLAME TIP TEMPERATURE CALCULATION

Fuel Volatiles	Stoichiometric Oxygen-Fuel Mass Ratio γ	Heat of Combustion Q_c (cal/g)	Fraction of Heat Loss by Radiation R_r	Source-Ambient Temperature Ratio T_o/T_a
Wood	1.1	2,500	0.3	1.9
City Gas	4.0	11,800	0.3	1.0
Ethane	3.7	11,300	0.3	1.0
n-Heptane	3.5	10,700	0.3	1.6

ILLUSTRATIONS

Figure 1 Turbulent Buoyant Diffusion Flame with a Differential Volume Element.

Figure 2 Correlation of Flame Height, Burning Rate, and Source Characteristics for Various Fuels.

Figure 3 Comparison of Predicted and Measured Gas Temperature along the Flame Axis of a Crib Fire. Width of the Crib- 0.559 m, fuel burning rate - 593 g/min., ambient temperature - 298°K, heat of combustion - 2500 cal/g., fraction of radiation loss - 0.35, entrainment coefficients - E=0.18 for the combustion zone, and E'=0.07 for the buoyant plume.

Figure 4 Comparison of Predicted and Measured Gas Temperature Distribution in the Vertical Direction for n - Heptane fire. Experimental data by Tarifa et al. (8), fuel burning rate - 5.32×10^{-3} g/cm^2-sec, ambient temperature - 293°K, heat of combustion - 10700 cal/g, fraction of radiation loss - 0.5, pan diameter - 0.25 m, entrainment coefficients - E=0.25 for the combustion zone, and E'=0.05 for the buoyant plume.

Figure 5 Molecular Weight and Concentration Distributions Along the Flame Axis for Crib Fire.

Figure 6 Molecular Weight and Concentration Distributions Along the Flame Axis for n - Heptane Fire.

ACKNOWLEDGEMENTS

The author wishes to acknowledge the assistance of Mr. C. F. Viertz with the experimental work. This work was supported by the United States Department of Housing and Urban Development.

Nomenclature

C_p heat capacity

E entrainment coefficient of the ambient air to the combustion zone

E' entrainment coefficient of the ambient air to the buoyant plume

F_r Froude nunber = $\frac{u_o^2}{g Y_o}$

F_s $\frac{u_s^2}{g Y_s}$

g gravitational constant

g_i production rate of i-th species per unit volume

G_i $\frac{g_i Y_o}{\rho_a u_o}$

H flame height

H_s height of the flame within the combustion zone

M molecular weight

$\dot{m}$ mass flow rate of volatile fuel per unit source area

M_c molecular weight of the flame gas in the combustion zone

N_b modified Froude number = $\frac{\dot{m}}{\rho_a \sqrt{g Y_o}}$

P pressure

Q_c net heat of combustion of volatile fuel

R universal gas constant

T absolute temperature

u axial velocity of the flame gas

v' dimensionless volumetric flow rate in the combustion zone

v^* dimensionless volumetric flow rate in the buoyant plume

w' dimensionless momentum flux in the combustion zone

w^* dimensionless momentum flux in the buoyant plume

x_i mass fraction of species i

Y flame radius or half-width

z distance along the flame axis

γ stoichiometric oxygen to fuel mass ratio $= \frac{\mu_o}{\mu_f}$

μ_i stoichiometric coefficient of species i

ν_i stoichiometric ratio

ρ density

ω $\left(\frac{\bar{M}_c}{M_a}\right)\Big/\left(1+\frac{Q_c x_{oa}}{\gamma C_p T_a}\right)$

Subscripts and Superscripts

a denotes ambient properties

f denotes volatile fuel

O denotes oxygen

N denotes nitrogen

o denotes fluid properties at the flame source

p denotes combustion products

s denotes fluid properties at the point of stoichiometric mixing

t denotes flame properties at the flame tip

$1/*$ denotes quantity have been made dimensionless

absence of any scripts denotes the flame properties

REFERENCES

1. Gross, D., and Fang, J. B., Performance Concept in Buildings, Joint RILEM-ASTM-CIB Symposium Proceedings, NBS Special Publication 361 (1972), Vol. 1, p. 677.
2. Thomas, P. H., Ninth Symposium (International) on Combustion, The Combustion Institute, Pittsburgh, Pa., (1963), p. 844.
3. Thomas, P. H., Baldwin R., and Heselden, A. J. M., Tenth Symposium (International) on Combustion, The Combustion Institute, Pittsburgh, Pa. (1963), p. 867.
4. Putnam, A. A., and Speich, C. F., Ninth Symposium (International) on Combustion, The Combustion Institute, Pittsburgh, Pa., (1963), p. 867.
5. Putnam, A.,A., and Speich, C. F., A Model Study of the Interaction Effects of Mass Fires, Summary Report No. 2 for Office of Civil Defense through National Bureau of Standards, NBS Contract CST-717, Battelle Memorial Institute, Columbus, Ohio, March 27, (1963).
6. Gross, D., J. Res. Nat. Bur. Stand. (U.S.) 66C(2),(1962), p. 99.
7. Fons, W. L., Clements, H. B., Elliott, E., R., and George, P. M., Project Fire Model, Summary Progress Report II, U. S. Forest Service, Southeastern Forest Experiment Station, Macon, Georgia (1962).
8. Tarifa, C. S., Natario, P. P., and Valdes, E. C., Open

Fires, Final Report for U. S. Forest Service under Grant FG-SP-114 and FG-SP-146, (1967).

9. Grinberg, I. M., and Putnam, A. A., A Model Study of the Interaction Effects of Mass Fires, Summary Report No. 3 for Office of Civil Defense through National Bureau of Standards, Battelle Memorial Institute, Columbus, Ohio, September 28 (1964).

10. Masliyah, J. H., and Steward, F. R., Combustion and Flame, 13, 613 (1969).

11. Nielson, H. J., and Tao, L. N., Tenth Symposium (International) on Combustion, The Combustion Institute, Pittsburch, Pa. (1965) p. 965.

12. Steward, F. R., Combustion and Flame, 8, 171 (1964)

13. Steward, F. R., Combustion Science and Technology, 2, 203 (1970).

14. Lee, S. L., and Emmons, H. W., J. Fluid Mech., 11, 353 (1961)

15. Morton, B. R., Taylor, G. I., and Turner, J. S., Proc. Roy. Soc. A 234, 1 (1956).

16. Rouse, H., Yih, C. S., and Humphreys, H. W., Tellus, 4, 201 (1952).

17. Alpert, R. L., Fire Induced Turbulent Ceiling-Jet, Technical Report FMRC Serial No. 19722-2, Factory Mutual Research Corporation, Norwood, Massachusetts, (1971).

18. Rao, V. K., and Brzustowski, T. A., Combustion Science and Technology, 1, 171 (1969).

19. Faure, H., The Use of Models in Fire Research, Publication No. 786, Natin
tion No. 786, National Academy of Sciences, National Research Council, Washington, D.C. (1961), p. 50.

20. Lee, S. L., and Ling, C. H., Eleventh Symposium (International) on Combustion, The Combustion Institute, Pittsburgh, Pa. (1967), p. 501.

21. Ricou, F. P., and Spalding, D. B., J. Fluid Mech., 11, 21 (1961).

22. Townsend, A.A., ibid., 26, 689 (1966).

23. Murgai, M. P., and Emmons, W. H., ibid, 8, 611 (1960).

24. Murgai, M. P., and Varma, R.K., Int. J. Heat Mass Transfer, 8, 833 (1965).

25. Varma, R. K., Murgai, M. P., and Ghildyal, C. D., Proc. Roy. Soc. (London) A314, 195 (1970).

26. Morton, B. R., Tenth Symposium (International) on Combustion, The Combustion Institute, Pittsburgh, Pa. (1965), p.973.

27. Smith, R.K., Eleventh Symposium (International) on Combustion, The Combustion Institute, Pittsburgh, Pa. (1967) p. 507.

28. Browne, F. L., Theories of the Combustion of Wood and Its Control - A Survey of the Literature, U. S. Forest Service, Research Paper FPL 19, Forest Products Laboratory, Madison, Wisconsin (1958).

29. Roberts, A. F., Combustion and Flame, 8, 345 (1964).

30. Kosdon, F. J., Williams, F. A., and Buman, C., Twelfth Symposium (International) on Combustion, The Combustion

Institute, Pittsburgh, Pa. (1969) p. 253.

31. Hill, B. J., J. Fluid Mech., 51, 773 (1972).

Appendix A

Solution of Equations Governing the Combustion Zone

Defining the following convenient variables of dimensionless volumetric flow rate and momentum flux:

For Axisymmetric Flow

$$v' = u' y'^2 \quad \text{and} \quad w' = \rho' u'^2 y'^2$$

For Two Dimensional Flow

$$v' = u' y' \quad \text{and} \quad w' = \rho' u'^2 y' \tag{A-1}$$

and substituting into the appropriate dimensionless continuity equation and equations of conservation of species, momentum, and energy (15-22) gives

Axisymmetric Flow

$$\frac{d(\rho' v')}{dz'} = 2E\sqrt{w'} \tag{A-2}$$

$$\frac{d(\rho' v' x_i)}{dz'} = \frac{G_i \rho' v'^2}{w'} + 2E\sqrt{w'}\, x_{ia} \tag{A-3}$$

$$\frac{dw'}{dz'} = \frac{(1-\rho')}{F_r}\,\frac{\rho' v'^2}{w'} \tag{A-4}$$

$$\frac{dv'}{dz'} = \frac{2E}{\omega}\sqrt{w'} \tag{A-5}$$

Two-Dimensional Flow

$$\frac{d(\rho' v')}{dz'} = \frac{E w'}{v'\sqrt{\rho'}} \tag{A-2}$$

$$\frac{d(\rho' v' x_i)}{dz'} = \frac{G_i \rho' v'^2}{w'} + \frac{E w' x_{ia}}{v' \sqrt{\rho'}} \tag{A-3}$$

$$\frac{dw'}{dz'} = \frac{(1-\rho')}{Fr} \frac{\rho' v'^2}{w'} \tag{A-4}$$

$$\frac{dv'}{dz'} = \frac{E w'}{\omega v' \sqrt{\rho'}} \tag{A-5}$$

subject to the boundary conditions at the flame base

$$w' = \rho_o', \quad v' = 1, \quad \rho' = \rho_o', \quad x_i = x_{io} \text{ and } z' = 0 \tag{A-6}$$

Division of equation (A-2) with equation (A-5)and integrating the resulting equation within the proper limits yields

$$\rho' v' = \rho_o' + \omega (v' - 1) \tag{A-7}$$

The entrainment coefficient in equation (A-3) may be eliminated by substitution of equation (A-2) into equation (A-3) and integration of the resultant equation with respect to axial distance gives the mass flux of species at height , in terms of the mass flux through the flame base, the rate of production due to chemical reaction and the mass flux entraining from the surrounding atmosphere:

$$x_i \rho' v' = x_{io} \rho_o' + \int_0^{z'} G_i \left(\frac{\rho' v'^2}{w'}\right) dz' + x_{ia} (\rho' v' - \rho_o') \tag{A-8}$$

Combustion reactions are generally quite complex, typically involving a multistep path with a number of short lived species. However, until detailed mixing and combustion data are available, it is assumed that chemical reaction can be idealized as a single step overall reaction.

$$\nu_f(\text{FUEL}) + \nu_o(\text{OXYGEN}) \longrightarrow \nu_p(\text{COMBUSTION PRODUCTS}) \quad \text{(A-9)}$$

and that the kinetics of the combustion process are fast enough that the reaction rate is controlled by the rate of oxygen entrained into the flame.

With these assumptions, the rates of production or comsumption of the species are determined by the stoichiometric coefficients for the overall reaction

$$\frac{g_f}{\mu_f} = \frac{g_o}{\mu_o} = -\frac{g_p}{\mu_p} \quad \text{(A-10)}$$

where $\mu_i = \nu_i M_i$, stoichiometric coefficient.

Because there is no excess oxygen within the combustion zone, equation A-8 for oxygen is expressed by

$$\int_0^{z'} G_o \left(\frac{\rho' v'^2}{w'}\right) dz' = -x_{oa}(\rho' v' - \rho_o') \quad \text{(A-11)}$$

For the concentration distribution of combustible volatiles, equation A-8 becomes

$$x_f \rho' v' = x_{fo} \rho_o' + \int_0^{z'} G_f \left(\frac{\rho' v'^2}{w'}\right) dz' \quad \text{(A-12)}$$

Introduction of the relations indicated by equations A-10 and A-11 into equation A-12 and using the definition of stoichiometric oxygen to combustible volatiles mass ratio, γ, gives

$$x_f \rho' v' = x_{fo} \rho_o' - \frac{x_{oa}}{\gamma}(\rho' v' - \rho_o') \quad \text{(A-13)}$$

where $\gamma = \frac{\mu_o}{\mu_f}$, the mass ratio of stoichiometric oxygen to combustion volatiles.

The mass flow rates at which the combustible volatiles are entirely consumed through chemical reaction with the oxygen entrained can be determined by setting the fuel concentration equal to zero in equation A-13.

$$\rho_s' v_s' = \rho_o' \left(1 + \frac{\gamma x_{so}}{x_{oa}}\right) \tag{A-14}$$

The dimensionless volumetric flow at stoichiometric mixing can be obtained through this relation in conjunction with Equation (A-7) evaluated at stoichiometric mixing.

$$v_s' = \frac{\rho_o' \left(\frac{\omega}{\rho_o'} + \frac{\gamma x_{so}}{x_{oa}}\right)}{\omega} \tag{A-15}$$

Using the relation given by equation (A-7) to eliminate ρ' in equation A-4 and dividing the resulting equation A-5 yields a total differential equation, as follows:

For Axisymmetric Flow

$$\frac{dw'}{dv'} = \left\{\frac{\omega}{2E F_r w'^{3/2}}\right\}\left\{v' - \left[\rho_o' + \omega(v'-1)\right]\right\}\left\{\rho_o' + \omega(v'-1)\right\}$$

For Two Dimensional Flow

$$\frac{dw'}{dv'} = \left\{\frac{\omega}{E F_r w'^2}\right\}\left\{\left[\omega v' + (\rho_o' - \omega)\right]^3 v'\right\}^{\frac{1}{2}}\left\{(1-\omega)v' + \omega - \rho_o'\right\} \tag{A-16}$$

Separation of variables and integration over the proper limits yields:

For Axisymmetric Flow

$$\frac{2}{5}(w'^{\frac{5}{2}} - \rho_o'^{\frac{5}{2}}) = \frac{\omega}{2EF_r}\left\{\frac{\omega(1-\omega)v'^3}{3} + \frac{(1-2\omega)(\rho_o'-\omega)v'^2}{2} - (\rho_o'-\omega)^2 v' - \left[\frac{\omega(1-\omega)}{3} - \frac{(1-2\omega)(\rho_o'-\omega)}{2} - (\rho_o'-\omega)^2\right]\right\}$$

For Two Dimensional Flow

$$\frac{1}{3}(w'^3 - \rho_o'^3) = \frac{\omega}{EF_r}\left\{ \frac{(1-\omega)}{4}\left[(v' + \frac{\rho_o'-\omega}{2\omega})\left(\omega v'^2 + (\rho_o'-\omega)v'\right)^{\frac{1}{2}}\right.\right.$$

$$\left(\omega v'^2 + (\rho_o'-\omega)v' - \frac{3(\rho_o'-\omega)^2}{8\omega}\right) + \frac{3(\rho_o'-\omega)^4}{32\omega^{5/2}} \ln\left(v' + \frac{\rho_o'-\omega}{2\omega} + \sqrt{v'^2 + \frac{\rho_o'-\omega}{\omega}v'}\right)\Big]$$

$$+ \frac{(\omega-\rho_o')}{3}\left[(\omega v' + \rho_o' - \omega)^{\frac{1}{2}}(\omega v')^{\frac{3}{2}}\left(\omega v' + \frac{7}{4}(\rho_o'-\omega)\right)\right.$$

$$+ \frac{3}{8}(\rho_o'-\omega)^2(\omega v')^{\frac{1}{2}}(\omega v' + \rho_o' - \omega)^{\frac{1}{2}}$$

$$\left. - \frac{3(\rho_o'-\omega)^3}{8} \ln\left(\frac{\sqrt{\omega v' + \rho_o' - \omega} + \sqrt{\omega v'}}{\sqrt{\rho_o'-\omega}}\right)\right]$$

$$- \frac{(1-\omega)}{4}\left[\left(\frac{\rho_o'^{\frac{1}{2}}(\rho_o'+\omega)}{2\omega}\right)\left(\rho_o' - \frac{3(\rho_o'-\omega)^2}{8}\right)\right.$$

$$\left. + \frac{3(\rho_o'-\omega)^4}{32\omega^{5/2}} \ln\left(\frac{\rho_o'+\omega}{2\omega} + \sqrt{\frac{\rho_o'}{\omega}}\right)\right]$$

$$- \frac{(\omega-\rho_o')}{3}\left[\rho_o'^{\frac{1}{2}}\omega^{\frac{3}{2}}\left(\frac{7}{4}\rho_o' - \frac{3}{4}\omega\right) + \frac{3}{8}(\rho_o'-\omega)^2(\rho_o'\omega)^{\frac{1}{2}}\right.$$

$$\left.\left. - \frac{3(\rho_o'-\omega)^3}{8} \ln\left(\frac{\sqrt{\rho_o'} + \sqrt{\omega}}{\sqrt{\rho_o'-\omega}}\right)\right]\right\}$$

(A-17)

In order to obtain a simplified functional relationship for further analysis, it is assumed that the volumetric flow rate at the flame base is negligible compared with that at stoichiometric mixing and that the velocity developed within the flame plume is much greater than that at the flame base.

With these assumptions, equation A-17 reduces to

For Axisymmetric Flow

$$w' = \left[\frac{5\omega^2(1-\omega)v'^3}{12\,E\,Fr}\right]^{\frac{2}{5}}$$

For Two Dimensional Flow

$$w' = \left[\frac{3\omega^{\frac{5}{2}}(1-\omega)v'^4}{4EFr}\right]^{\frac{1}{3}} \qquad \text{(A-18)}$$

Introduction of this relation into equation A-5 and integrating the resulting equation yields the flame height measured from the flame base up to stoichiometric mixing point. These equations are:

For Axisymmetric Flow

$$\frac{H_s}{Y_o} = \frac{5\omega}{4E}\left[\frac{12\,E\,Fr}{5\,\omega^2(1-\omega)}\right]^{\frac{1}{5}}\left[v_s'^{\frac{2}{5}} - 1\right]$$

For Two Dimensional Flow

$$\frac{H_s}{Y_o} = \left[\frac{9\omega^2 Fr}{2E^2(1-\omega)}\right]^{\frac{1}{3}}\left[v_s'^{\frac{2}{3}} - 1\right] \qquad \text{(A-19)}$$

Substitution for F_r and v_s' and introducing the total mass flux entering through the flame base

$$\dot{m} = \rho_o u_o \qquad \text{(A-20)}$$

into equation A-19 while neglecting unity compared with v_s' term produces the desired result (equation 24).

Integration of equation A-5 after substitution for w' from equation A-18 yields

For Axisymmetric Flow

$$v' = \left\{ \frac{4Ez'}{5} \left[\frac{5(1-\omega)}{12E\omega^3 Fr} \right]^{\frac{1}{5}} + 1 \right\}^{\frac{5}{2}}$$

For Two Dimensional Flow

$$v' = \left\{ \left[\frac{2E^2(1-\omega)}{9\omega^2 Fr} \right]^{\frac{1}{3}} z' + 1 \right\}^{\frac{3}{2}} \qquad \text{(A-21)}$$

The flame radius divided by its source radius can be obtained by a combination of the definitions of dimensionless volumetric flow rate and momentum flux:

For Axisymmetric Flow

$$Y' = \frac{\sqrt{\rho'}\, v'}{\sqrt{w'}}$$

For Two Dimensional Case

$$Y' = \frac{\rho' v'^2}{w'} \qquad \text{(A-22)}$$

Substitution for $\rho' v'$, w' and v' from equations A-7, A-18, and A-21 into the above equation yields the desired equation 25. Equation 26 is obtained from equation 22 evaluated at stoichiometric mixing and substitution for $\rho_s' v_s'$, v_s' and w_s' from equations A-14, A-15, and A-18.

The dimensionless density of the flame plume (equation 27) is obtained from equation A-7 in which v' is replaced by the

relation given by equation A-21.

Division of equation A-14 by equation A-15 yields the desired equation 28.

An overall energy balance on the entire combustion zone from the flame base up to the stoichiometric mixing height results in

$$T_s' = \frac{1}{\omega}\left[\frac{\rho_o'(\omega T_o' - 1)}{\rho_s' v_s'} + 1\right] \qquad \text{(A-23)}$$

Substitution for $\rho_s' v_s'$ from equation A-14 into equation A-23 and rearranging yields the desired result, equation 30. Rearrangement of equation A-13 and substitution for $\rho' v'$ and v' from equations A-7 and A-21 gives the desired equation 31. Substituting equation A-7 and A-21 into equation A-8 for the combustion products and simplifying the resulting equation with use of equations A-10 and A-11 yields the desired equation 32.

Neglecting the species generation term in equation A-8 for nitrogen and replacement of $\rho' v'$ and v' with equation A-7 and A-21 yields the desired result, equation 33.

The total mass flow rate of combustion products across a plane at the stoichiometric mixing height is equal to the mass rate supplied to the flame base plus the mass rate entrained from the ambient atmosphere plus the mass flux generated by combustion. This relationship is expressed as:

$$x_{ps} = \frac{x_{pa}(\rho_s' v_s' - \rho_o') + \rho_o'(x_{po} + x_{so}\frac{\mu_p}{\mu_s})}{\rho_s' v_s'} \qquad \text{(A-24)}$$

Substituting for $\rho_s' v_s'$ from equation A-14 into equation A-24 yields the desired resultant equation 34.

An overall mass balance for nitrogen on the whole combustion zone, substitution for $\rho_s' v_s'$ from equation A-14 and rearrangement of the resulting equation gives the desired equation 35.

Appendix B

Solution of Governing Equations in the Buoyant Plume

Introduction of the simplifying variables of dimensionless volumetric flow rate and momentum flux

For Axisymmetric Flow

$$v^* = u^* y^{*2} \quad \text{and} \quad w^* = \rho' u^{*2} y^{*2}$$

For Two Dimensional Flow

$$v^* = u^* y^* \quad \text{and} \quad w^* = \rho' u^{*2} y^* \tag{B-1}$$

into the equations of conservation of mass, species, momentum, and energy yields:

Axisymmetric Flow

$$\frac{d(\rho' v^*)}{dz^*} = 2E'\sqrt{w^*} \tag{B-2}$$

$$\frac{d(\rho' v^* x_i)}{dz^*} = 2E'\sqrt{w^*}\, x_{ia} \tag{B-3}$$

$$\frac{dw^*}{dz^*} = \frac{(1-\rho')}{F_s}\frac{\rho' v^{*2}}{w^*} \tag{B-4}$$

$$\frac{dv^*}{dz^*} = 2E'\sqrt{w^*} \tag{B-5}$$

Two Dimensional Flow

$$\frac{d(\rho' v^*)}{dz^*} = \frac{E' w^*}{v^*\sqrt{\rho'}} \tag{B-2}$$

$$\frac{d(\rho' v^* x_i)}{dz^*} = \frac{E' w^* x_{ia}}{v^* \sqrt{\rho'}} \tag{B-3}$$

$$\frac{dw^*}{dz^*} = \frac{(1-\rho')}{F_s} \frac{\rho' v^{*2}}{w^*} \tag{B-4}$$

$$\frac{dv^*}{dz^*} = \frac{E' w^*}{v^* \sqrt{\rho'}} \tag{B-5}$$

The boundary conditions at the source of the buoyant plume zone are

$$w^* = \rho_s', \; v^* = 1, \; \rho' = \rho_s', \; x_i = x_{is} \quad \text{at} \quad z^* = z_s^* \tag{B-6}$$

Dividing equation B-2 with equation B-5 and integrating between the pertinent limits results in:

$$\rho' v^* = \rho_s' + (v^* - 1) \tag{B-7}$$

Using equation B-5 to divide equation B-4 and eliminating ρ' between the resultant equation and equation B-7, one obtains

For Axisymmetric Flow

$$\frac{dw^*}{dv^*} = \left[\frac{1}{2E' F_s w^{*3/2}}\right]\left[1-\rho_s'\right]\left[v^* + (\rho_s' - 1)\right]$$

For Two Dimensional Flow

$$\frac{dw^*}{dv^*} = \left[\frac{v^{*\frac{1}{2}}}{E' F_s w^{*2}}\right]\left[1-\rho_s'\right]\left[v^* + (\rho_s' - 1)\right] \tag{B-8}$$

Separation of variables and integration yields:

For Axisymmetric Flow

$$\frac{2}{5}\left(w^{*\frac{5}{2}} - \rho_s'^{\frac{5}{2}}\right) = \frac{(1-\rho_s')}{2E' F_s}\left[\frac{v^{*2}}{2} + (\rho_s' - 1)v^* - (\rho_s' - \tfrac{1}{2})\right]$$

For Two Dimensional Flow

$$\frac{1}{3}(w^{*3} - \rho_s'^3) = \frac{(1-\rho_s')}{3E'F_s}\left\{v^{*\frac{3}{2}}(v^* + \rho_s' - 1)^{\frac{1}{2}}\left[v^* + \frac{7}{4}(\rho_s' - 1)\right]\right.$$

$$+ \frac{3}{8}(\rho_s'-1)^2(v^* - \rho_s' - 1)^{\frac{1}{2}}v^{*\frac{1}{2}} - \frac{3(\rho_s'-1)^3}{8}\ln\left(\frac{\sqrt{v^*+\rho_s'-1} + \sqrt{v^*}}{\sqrt{\rho_s'-1}}\right)$$

$$\left.-\left[\rho_s'^{\frac{1}{2}}\left(\frac{7}{4}\rho_s' - \frac{3}{4}\right) + \frac{3}{8}(\rho_s'-1)^2\rho_s'^{\frac{1}{2}} - \frac{3(\rho_s'-1)^3}{8}\ln\left(\frac{\sqrt{\rho_s'}+1}{\sqrt{\rho_s'-1}}\right)\right]\right\}$$

(B-9)

In order to proceed to further analytical treatment, it may be possible to neglect ρ_s' compared with w^* for points far from the source and to retain the term containing the highest power of v^* . This approximation yields the following:

For Axisymmetric Flow

$$w^* = \left[\frac{5(1-\rho_s')v^{*2}}{8E'F_s}\right]^{\frac{2}{5}}$$

For Two Dimensional Flow

$$w^* = \left[\frac{(1-\rho_s')v^{*3}}{E'F_s}\right]^{\frac{1}{3}} \qquad \text{(B-10)}$$

Substituting this relation for w^* into equation B-5 and integrating the resulting equation, one obtains the total flame height

For Axisymmetric Flow

$$H^* = H_s^* + \frac{5}{6E'}\left[\frac{8E'F_s}{5(1-\rho_s')}\right]^{\frac{1}{5}}\left[v^{*\frac{3}{5}} - 1\right]$$

For Two Dimensional Flow

$$H^* = H_s^* + \left[\frac{F_s}{E'^2(1-\rho_s')}\right]^{\frac{1}{3}} \left\{\left[v_t^{*2} + (\rho_s'-1)v_t^*\right]^{\frac{1}{2}} + (\rho_s'-1)\ln\left[v_t^{*\frac{1}{2}} + (v_t^* + \rho_s' - 1)^{\frac{1}{2}}\right] - \rho_s'^{\frac{1}{2}} + (1-\rho_s')\ln(1+\rho_s'^{\frac{1}{2}})\right\}$$

which is approximated by

$$H^* = H_s^* + \left[\frac{F_s}{E'^2(1-\rho_s')}\right]^{\frac{1}{3}} \left[v_t^* - 1\right] \qquad \text{(B-11)}$$

where $H^* = \frac{H}{Y_s}$ and $H_s^* = \frac{H_s}{Y_s}$

The dimensionless volumetric flow rate (v_t^*) at the flame tip can be obtained through an overall energy and mass balance on the entire convection plume along with using the assumption of identical heat for both plume gas and ambient fluid, such that:

$$v_t^* = \frac{T_t'(1-\rho_s') + (\rho_s' T_s' - 1)}{T_t' - 1} \qquad \text{(B-12)}$$

where $v_t^* = \frac{v_t}{v_s}$

Substitution for ρ_s' and T_s' from equations 28 and 30 into equation B-12 results in:

$$v_t^* = \frac{\left\{\left[\frac{\omega(1-\rho_o')}{\rho_o'} + \frac{\gamma x_{so}(1-\omega)}{x_{oa}}\right] T_t' + \frac{\omega(\rho_o' T_o' - 1)}{\rho_o'}\right\}}{\left(\frac{\omega}{\rho_o'} + \frac{\gamma x_{so}}{x_{oa}}\right)(T_t' - 1)} \qquad \text{(B-13)}$$

Introduction of the definition of Froude number F_s into equation B-11 while neglecting unity compared with v_t' because the volumetric flow rate at the flame tip is much greater than that at stoichiometric mixing yields:

For Axisymmetric Flow

$$\frac{H}{Y_0} = H_s' + 0.916 \left[\frac{v_s'^2 v_0^2}{E'^4 g Y_0^5 (1-\rho_s')} \right]^{\frac{1}{5}} v_t^{*\frac{3}{5}}$$

For Two Dimensional Flow

$$\frac{H}{Y_0} = H_s' + \left[\frac{v_s'^2 v_0^2}{E'^2 g Y_0^3 (1-\rho_s')} \right]^{\frac{1}{3}} v_t^* \qquad \text{(B-14)}$$

where $v_s' = \frac{v_s}{v_0}$, volumetric flow rate at stoichiometric mixing divided by that at the flame base.

Substituting for v_s' from equation A-15, ρ_s' from equation 28, v_t^* and H_s' from equations B-13 and 24 into equation B-14 along with the definition of mass flux of fuel supplied to the flame source (equation A-20) yields the desired result (equation 58).

Using equation B-10 to replace w^* in equation B-5 and integrating the resulting equation, one obtains

For Axisymmetric Flow

$$v^* = \left\{ \frac{6E'(z^* - z_s^*)}{5} \left[\frac{5(1-\rho_s')}{8E'F_s} \right]^{\frac{1}{5}} + 1 \right\}^{\frac{5}{3}}$$

For Two Dimenional Flow

$$v^* = \left\{ (z^* - z_s^*) \left[\frac{E'(1-\rho_s')}{F_s} \right]^{\frac{1}{3}} + 1 \right\} \qquad \text{(B-15)}$$

Substitution for $\rho' v^*, w^*$ and v^* from equation B-7, B-10, and B-15 into equation A-22 along with the definition of F_s and approximation of the resulting equation gives the desired equation 59.

Solving equation B-7 for ρ' and substituting for v^* from equation B-15 together with the definition of F_s gives the desired result, equation 60.

Dividing equation B-3 by equation B-2, separation of variables and integration between the proper limits yields:

$$x_i \rho' v^* = x_{is} \rho_s' + x_{ia}(\rho' v^* - \rho_s') \tag{B-16}$$

Elimination of $\rho' v^*$ between equation B-7 and B-16 for oxygen and substitution for v^* from equation B-15 gives the desired equation 62.

Equation 63 is obtained by a combination of equations B-7 and B-16 for combustion products with equation B-15.

Elimination of $\rho' v^*$ between equations B-7 and B-16 for nitrogen and substituting for v^* from equation B-15 yields the desired results, equation 64.

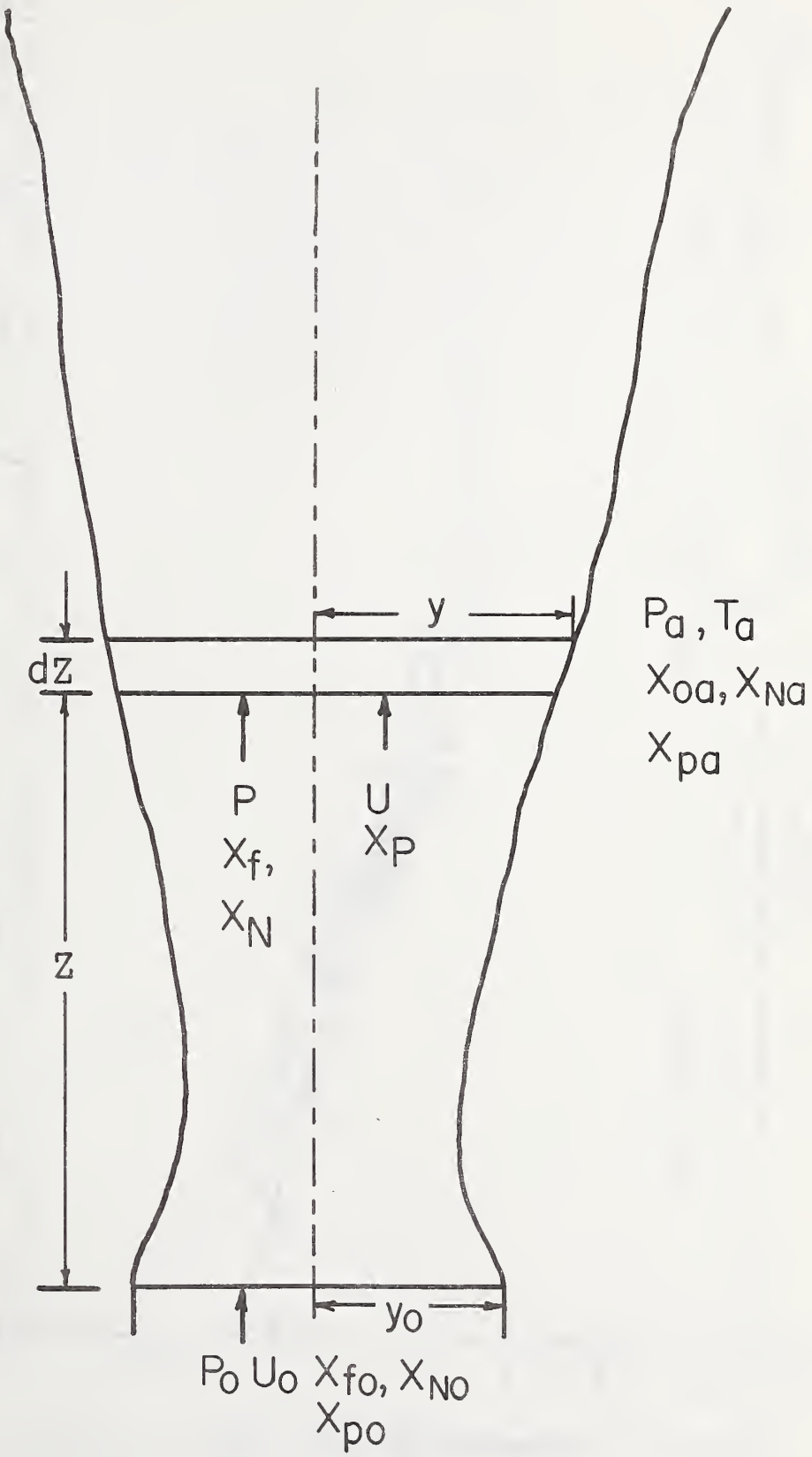

FIGURE 1

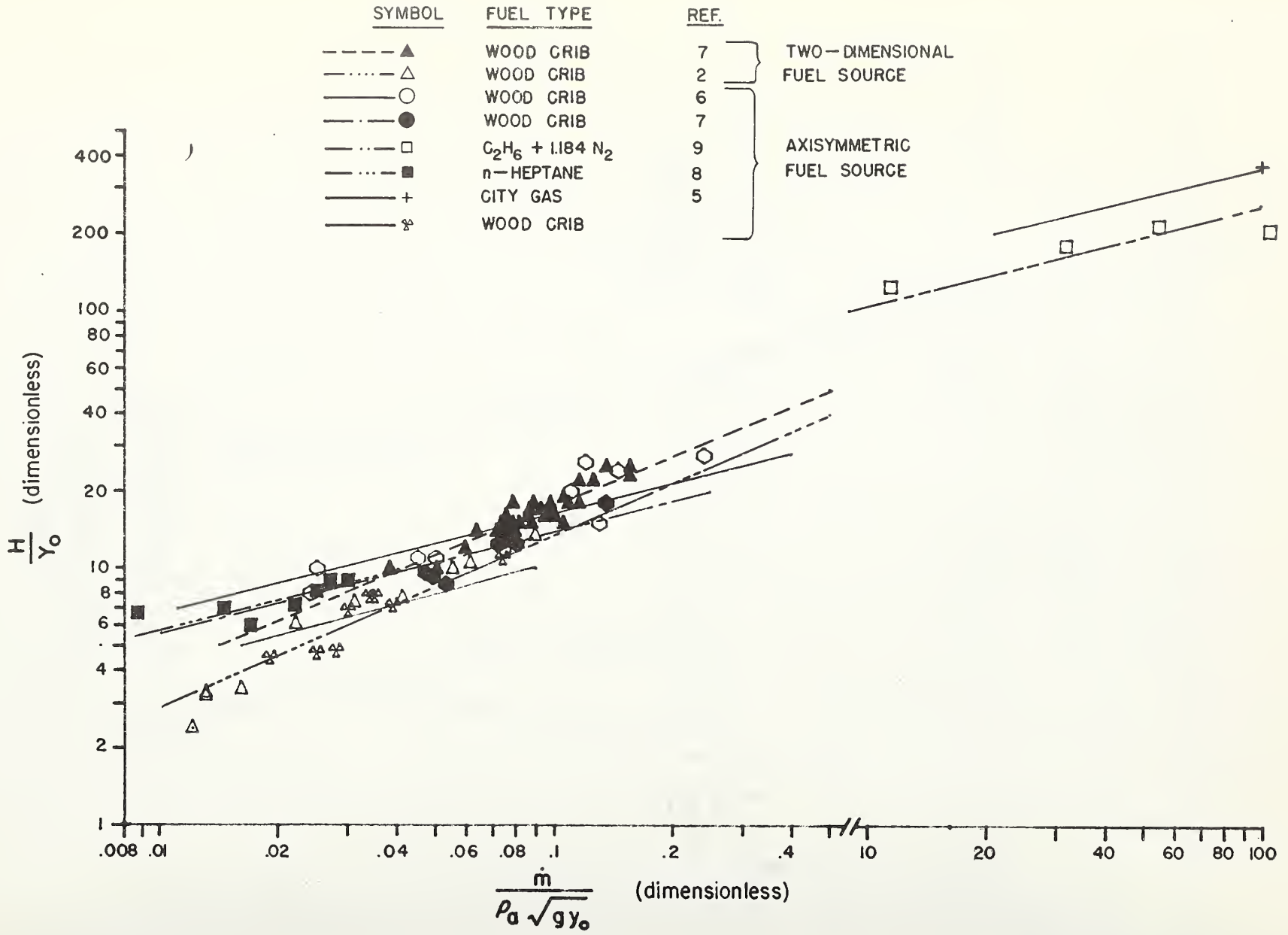
SYMBOL
FUEL TYPE
REF.
WOOD CRIB 7
WOOD CRIB 2
WOOD CRIB 6
WOOD CRIB 7
C_2H_6 + 1.184 N_2 9
n-HEPTANE 8
CITY GAS 5
WOOD CRIB
TWO-DIMENSIONAL FUEL SOURCE
AXISYMMETRIC FUEL SOURCE
$\frac{H}{Y_o}$ (dimensionless)
$\frac{\dot{m}}{\rho_a \sqrt{g y_o}}$ (dimensionless)
400
200
100
80
60
40
20
10
8
6
4
2
1
.008
.01
.02
.04
.06
.08
.1
.2
.4
10
20
40
60
80
100

FIGURE 2

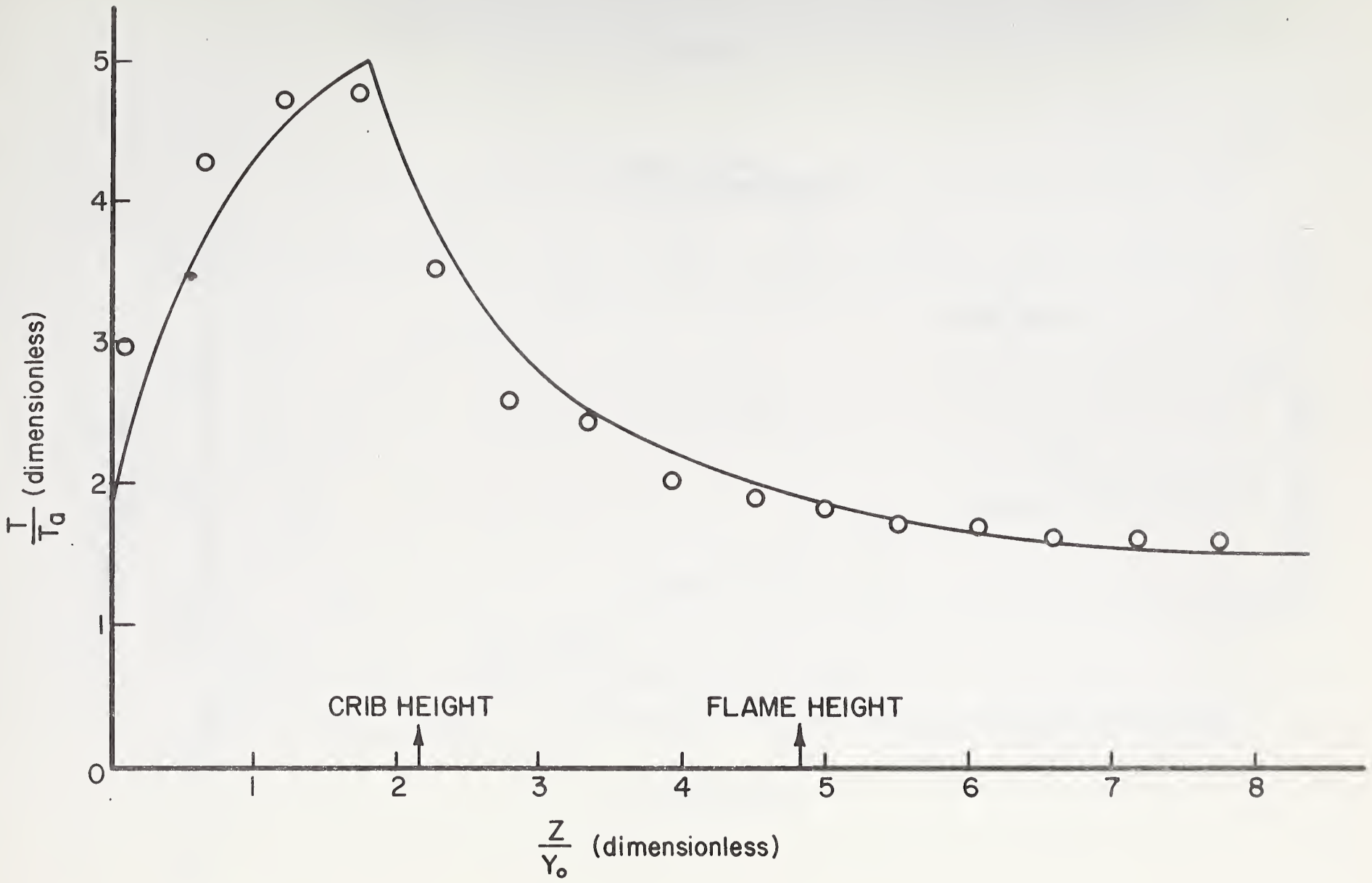
5
4
3
2
1
0
$\frac{T}{T_a}$ (dimensionless)
CRIB HEIGHT
FLAME HEIGHT
1
2
3
4
5
6
7
8
$\frac{Z}{Y_o}$ (dimensionless)

FIGURE 3

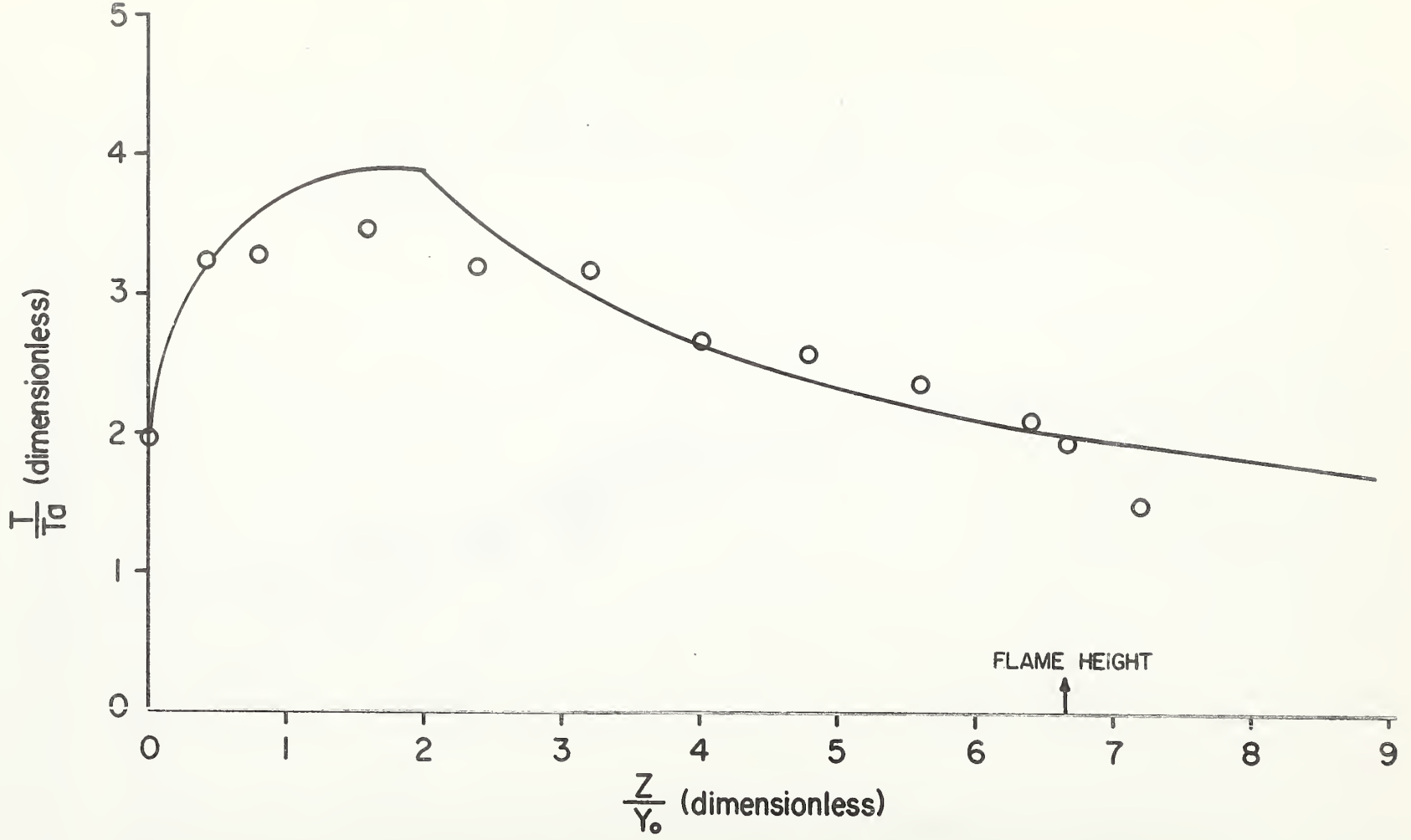
5
4
3
2
1
0
T/Ta (dimensionless)
FLAME HEIGHT
0
1
2
3
4
5
6
7
8
9
Z/Yo (dimensionless)

FIGURE 4

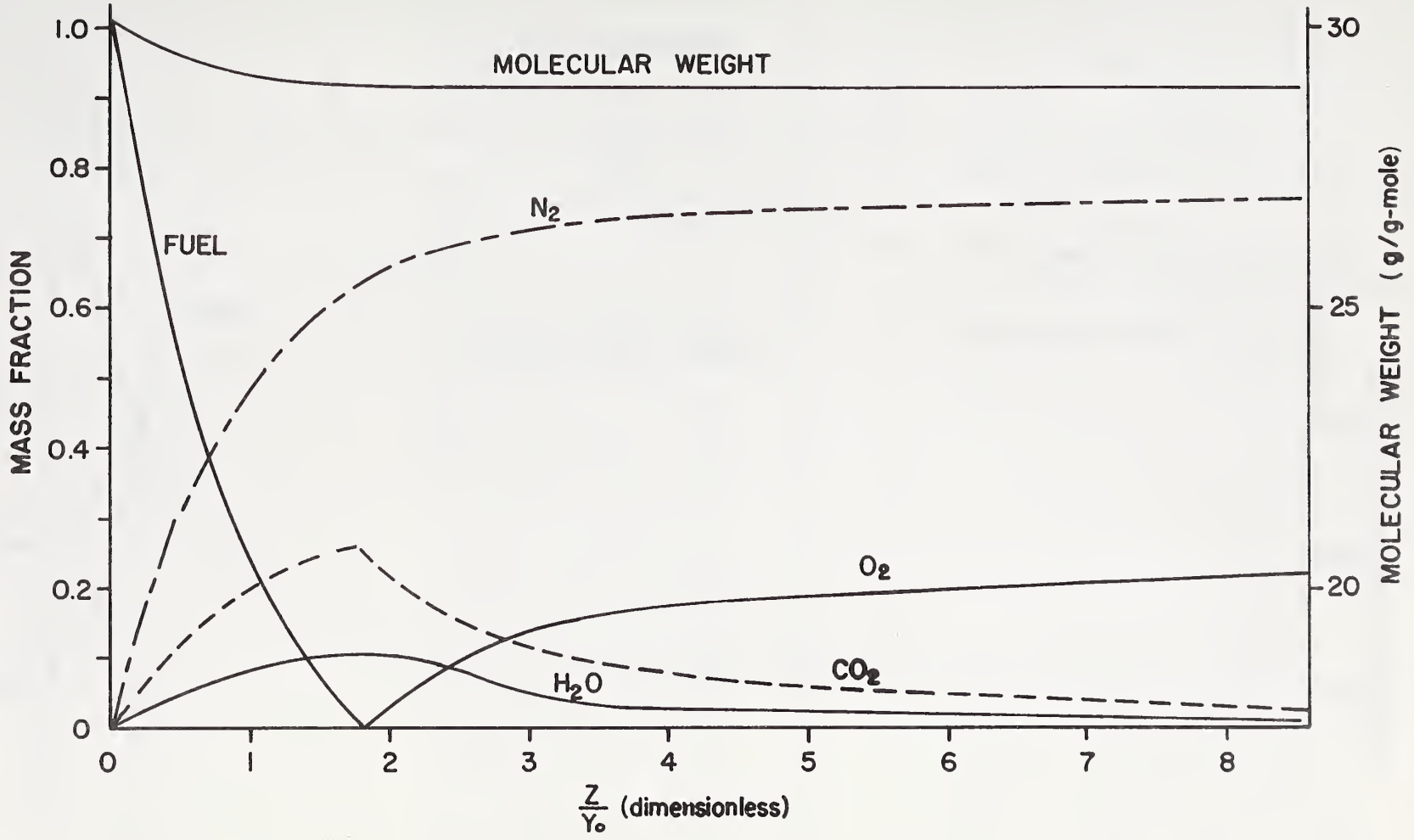
MOLECULAR WEIGHT
FUEL
N_2
O_2
CO_2
H_2O
MASS FRACTION
MOLECULAR WEIGHT (g/g-mole)
1.0
0.8
0.6
0.4
0.2
0
30
25
20
0
1
2
3
4
5
6
7
8
$\frac{Z}{Y_o}$ (dimensionless)

FIGURE 5

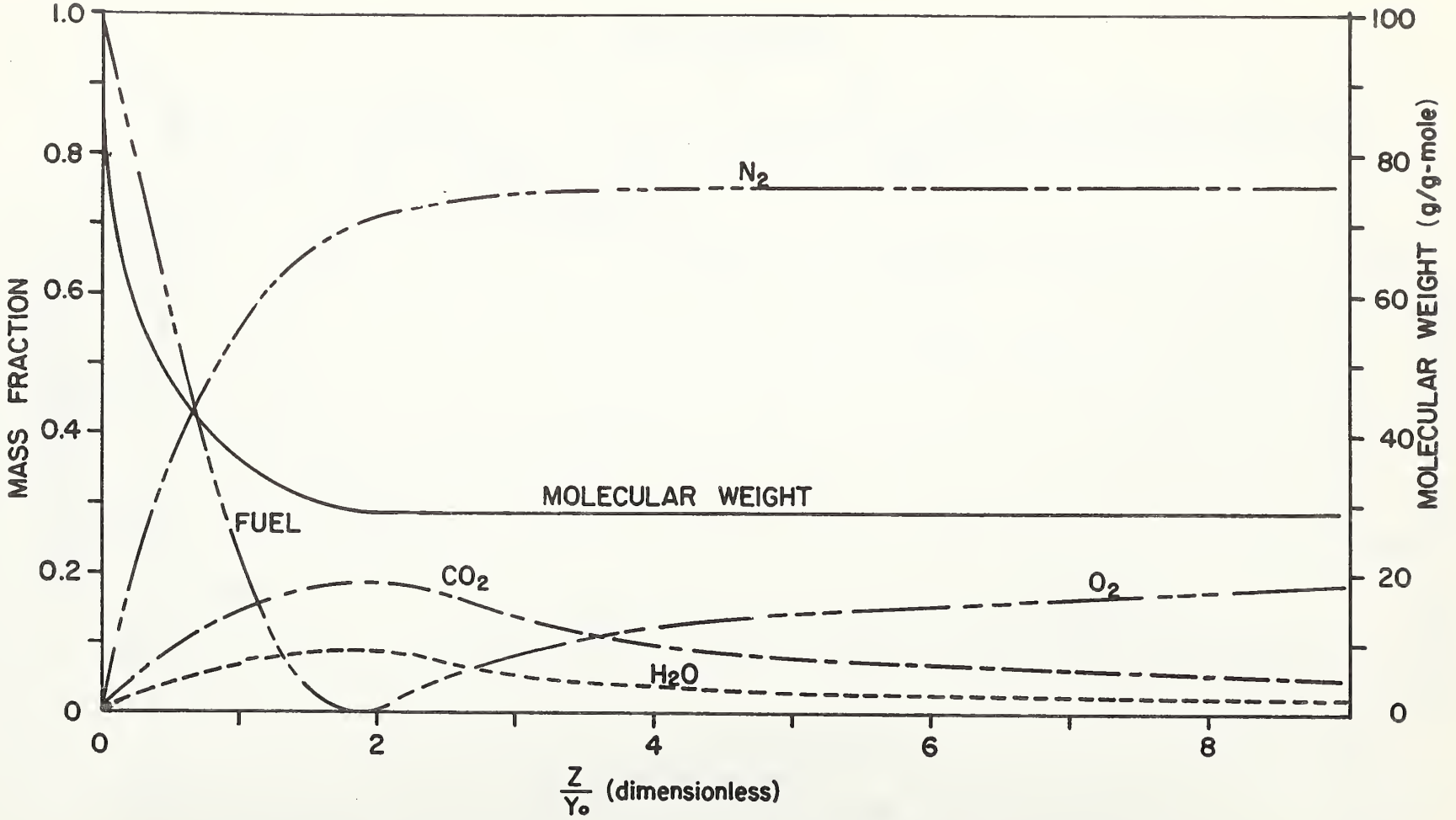
1.0
0.8
0.6
0.4
0.2
0
MASS FRACTION
100
80
60
40
20
0
MOLECULAR WEIGHT (g/g-mole)
N_2
MOLECULAR WEIGHT
FUEL
CO_2
O_2
H_2O
0
2
4
6
8
$\frac{Z}{Y_o}$ (dimensionless)

FIGURE 6

FORM NBS-114A (1-71)

U.S. DEPT. OF COMM. BIBLIOGRAPHIC DATA SHEET	1. PUBLICATION OR REPORT NO. NBSIR 73-115	2. Gov't Accession No.	3. Recipient's Accession No.

4. TITLE AND SUBTITLE

Analysis of the Behavior of a Freely Burning Fire in a Quiescent Atmosphere

5. Publication Date

6. Performing Organization Code

7. AUTHOR(S)

J. B. Fang

8. Performing Organization NBSIR 73-115

9. PERFORMING ORGANIZATION NAME AND ADDRESS

NATIONAL BUREAU OF STANDARDS
DEPARTMENT OF COMMERCE
WASHINGTON, D.C. 20234

10. Project/Task/Work Unit No. 4618382

11. Contract/Grant No. IAA-H-37-72 Amendment 10

12. Sponsoring Organization Name and Address

Department of Housing and Urban Development
Washington, D.C.

13. Type of Report & Period Covered Interim

14. Sponsoring Agency Code

15. SUPPLEMENTARY NOTES

16. ABSTRACT (A 200-word or less factual summary of most significant information. If document includes a significant bibliography or literature survey, mention it here.)

A mathematical model which describes the physical and geometrical properties of a turbulent buoyant diffusion flame over a free burning fire has been set up for both axisymmetric and two dimensional cases. The mathematical simulation of the flame consists of a combustion zone near its source and a buoyant plume above and has been developed based on the assumptions of infinitely rapid rate of oxygen limited combustion reaction and "top hat" profiles representing vertical distributions of the velocity, temperature, and concentration of the flame gas. Analytical solutions are presented showing the effects of fuel mass-flow rate, physical properties of the fuel and ambient air, and the size and shape of burning area on the general characteristics of a buoyant flame. Experimental data on visable flame heights and flame temperature profiles obtained from burning several different fuels have been satisfactorily correlated by the derived expressions.

17. KEY WORDS (Alphabetical order, separated by semicolons) buoyant plume; diffusion flame; fire; flame height; mathematical modeling; turbulent flow.

18. AVAILABILITY STATEMENT

XX UNLIMITED.

[ ] FOR OFFICIAL DISTRIBUTION. DO NOT RELEASE TO NTIS.

19. SECURITY CLASS (THIS REPORT)	21. NO. OF PAGES
UNCLASSIFIED	
20. SECURITY CLASS (THIS PAGE)	22. Price
UNCLASSIFIED	